PIEZOELECTRIC MICRO DITHER STAGE CALIBRATION OF 6-AXIS IMU

Visarute Pinrod, Sachin Nadig, Serhan Ardanuç, and Amit Lal
*Sonic*MEMS Laboratory, Department of Electrical and Computer Engineering
Cornell University, Ithaca, NY, USA

ABSTRACT

We demonstrate simultaneous extraction of the scale factor and cross axis sensitivity of a commercial 6-DOF Inertial Measurement Unit (IMU), which has three gyroscopes and three accelerometers, using a multi-axis, mm-scale piezoelectric dither stage. The stage is 25.4x25.4x0.5 mm, with a platform disk of diameter 7.5 mm, onto which the IMU chip is adhesively attached. The stage has small inertia allowing for high bandwidth on-the-fly calibration and tracking of scale factor drift using rotation dither rates and accelerations as high as 100 deg/sec and 90 m/s^2, respectively. We measure the gyroscope cross-axis sensitivities of 2.4%, which is within the IMU specifications. Using the cross-axis sensitivity and the scale factors, we demonstrate a pathway to improving commercial IMUs, reaching performance needed for personal navigation.

INTRODUCTION

High levels of electronics integration with MEMS inertial sensors have led to the System-on-a-Chip (SOC) sensor solutions, which bring together a 3-axis gyroscope, a 3-axis accelerometer, and sometimes a 3-axis magnetic sensor, and a barometric pressure sensor in a single low cost, low power and small IMU package [1]. These SOCs measure many useful quantities in handheld platforms, such as IMU assisted GPS navigation, and rate based motion assessment. Due to the non-zero bias and scale factor aging of the inertial sensors, consumer grade IMUs alone cannot be used for navigation for long durations [2]. This limitation can be overcome by incorporating a precise self-calibration system to continuously calibrate the sensors to obtain real time scale factor and bias. This would allow higher accuracies under large environmental variations and enable applications such as navigation in GPS-denied settings [3].

Available methods of self-calibration include direct electronic rate injection [4], application specific calibration algorithms [5-8], and integrated miniature high precision motion stages [9-12]. In some devices, the IMU chips have a self-test pin or a digital controlled self-test command that can check functionality and perform a self-calibration to extract scale factor [4]. However, this approach does not yield variation in cross-axis sensitivities. Application specific calibration algorithms work based on sensor fusion or output obtained from devices such as cameras [5], GPS units [6], barometric pressure sensors [7], and accelerometers measuring Earth's gravity [8]. However, incorporation of measurements from external sensors at high accuracies under varying conditions and locations is also challenging. Applying known external mechanical stimuli can be done by traditional bulky rate tables or integrated miniature high precision motion stages that do not disrupt their small form-factors [9-11].

In this paper, a micro dither stage, which is fabricated from a piezoelectric PZT plate, is used to apply acceleration in x (A_x), acceleration in y (A_y), and angular dither in z axis (Ω_z). Fabrication, operation, and characterization of a multi-axis piezoelectric dither platform using this stage was shown in [12], and calibration of a z-axis gyroscope using the same stage was presented in [10]. The dither stage provides precise measurements of instantaneous scale factor to within 700 ppm, which would enable long term monitoring of sensor biases and may enable navigation with the 6 DOF IMU chips. The stage is also compatible with optical readout schemes that allow closed-loop feedback for higher accuracy operation [13].

EXPERIMENTAL SETUP

Piezoelectric dither stage

The calibration system consists of a monolithic, planar, laser-micro machined PZT dither stage actuated by four PZT coiled bimorph cantilevers as shown in Figure 1a. The cross section of the bimorph cantilever with two electrodes on top and one electrode at the bottom is shown in Figure 1b [14]. Each cantilever coil can be actuated in different directions by controlling voltages on two top electrodes while grounding the bottom electrode. The top view of a cantilever going through in-plane bending is shown in Figure 1c. Undesired motion was suppressed by a spring connecting between the coil and the stage as shown in Figure 1d.

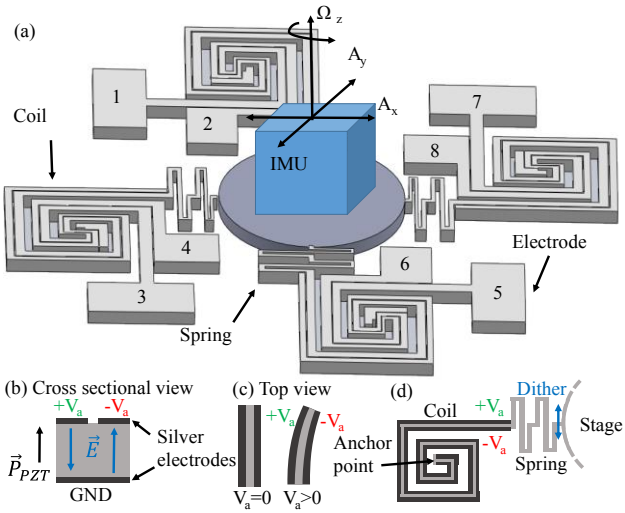

Figure 1. (a) 3D illustration of PZT dither stage with 8 electrodes for mechanical stimulate IMU in 3 modes (A_x, A_y, Ω_z) (b) Cross section of the PZT cantilever consist of connected ground electrode and separated top electrode (c) Top view of PZT cantilever (d) Coil and spring to actuate the stage

The PZT stage can dither in 3 modes (A_x, A_y, and Ω_z), which are controlled by the polarity of the voltage applied

on 8 electrodes as shown in Figure 2 and summarized in Table 1. The amplitudes of dither angular speed and acceleration are controlled by varying frequency of sine wave excitation to the stage at a fixed amplitude. The control of the frequency instead of amplitude decreases the piezoelectric polarization related nonlinearity of actuation under quasistatic operation and allows a large dynamic range of angular rate.

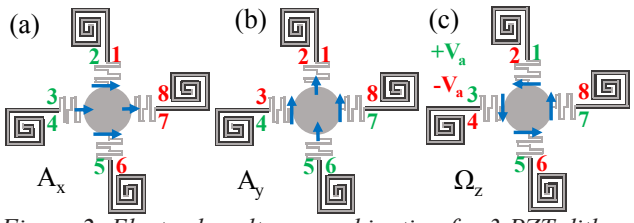

Figure 2: Electrode voltage combination for 3 PZT dither stage modes (a) A_x, (b) A_y, (c) Ω_z

Table 1: Electrode voltage combination for 3 PZT dither stage modes (A_x, A_y, Ω_z), for which actuator voltage is V_a. The electrode numbers are shown in Figure 2.

	Electrode							
Mode	**1**	**2**	**3**	**4**	**5**	**6**	**7**	**8**
A_x	$-V_a$	V_a	V_a	V_a	V_a	$-V_a$	$-V_a$	$-V_a$
A_y	$-V_a$	$-V_a$	$-V_a$	V_a	V_a	V_a	V_a	$-V_a$
Ω_z	V_a	$-V_a$	V_a	$-V_a$	V_a	$-V_a$	V_a	$-V_a$

Motherboard

Testing of the stage is done by mounting a 6 DOF IMU, MAX21105, upside down and wire bonding it to a jacket PCB as seen in Figure 3a. The block diagram of the system is shown in Figure 3b. The motherboard, which consists of waveform generators, voltage amplifiers, mechanical relays, and a microcontroller, is shown in Figure 3c.

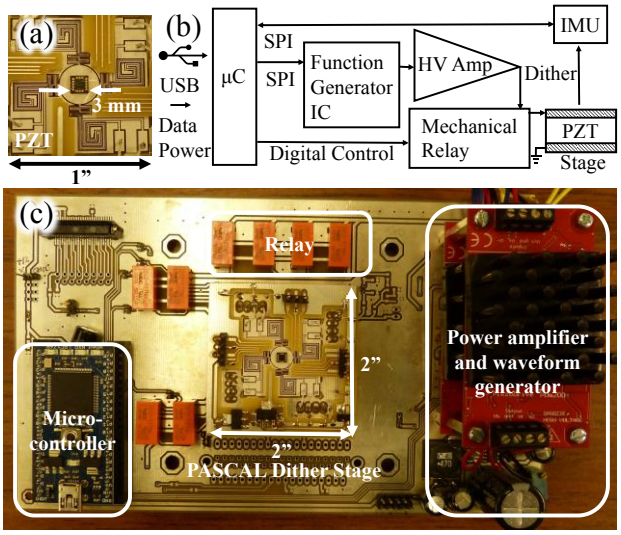

Figure 3: (a) 6-DOF IMU (MAX21105) mounted upside down on PZT dither stage (b) Block diagram and (c) Picture of the control board used to calibrate the IMU

AD9833 waveform generator, timed by CTS636 reference clock, generates a 0.6V_{pp} sine wave with 0.3 V_{DC} offset by direct digital synthesis (DDS). LC low pass filter removes high frequency quantization noise. Series of LM833 operational amplifiers creates two output voltages with the opposite polarity $V(t) = \pm 5V \sin(\omega t)$. Two PDM200 high performance piezo drivers amplify voltage to $V(t) = \pm 100V \sin(\omega t)$. The PZT stage electrodes connect to Kemet EC2 miniature dual coiled, latched signal relays to control polarity. An MBED microcontroller controls waveform generators and mechanical relays as it acquires 6-axis data with on-chip temperature from the IMU via SPI communication. The motherboard control and data acquisition to a computer is achieved in MATLAB software via a generic serial USB. The board, which has a size of 7.4" x 4.4", is compatible with a single 5V or 12 V power supply. The electronic control system has been assembled using of-the-shelf electronics, and can be greatly miniaturized using ASICs, to further reduce the size weight and power of the system.

STAGE CALIBRATION

The results of PZT stage calibration in 3 dither modes by a stroboscopic technique using Polytec MSA-400 microsystem analyzer is shown in Figure 4 for a stage holding the IMU chip with wirebonds. The stage scale factors are extracted by a linear fit for Ω_z mode, and a quadratic fit for A_x and A_y modes. Respective stage scale factors are given in Table 2.

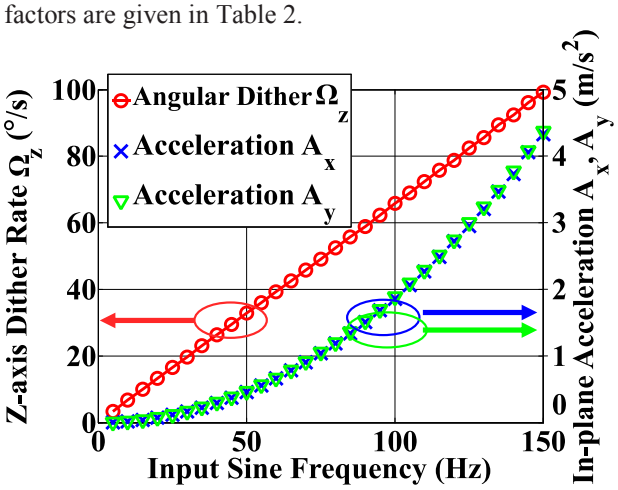

Figure 4: Loaded PZT stage response under 3 dither modes: (i) Rotational, (ii) X- translation, and (iii) Y-translation as measured by in-plane stroboscopy (Polytec MSA-400 Micro System Analyzer).

Table 2: Dither stage scale factor.

Dither Mode	**Stage scale factor**	**Unit**
X-axis acceleration (A_x)	201±3	$(\mu m/s^2)/Hz^2$
Y-axis acceleration (A_y)	202±3	$(\mu m/s^2)/Hz^2$
Z-axis rotation (Ω_z)	0.662±0.002	(Degree/s)/Hz

IMU CALIBRATION

IMU suffers from bias, scale factor, cross-coupling errors as well as random noise where the IMU output error model without nonlinearity is,

$$\vec{a}_{out} = \bar{M}_a \vec{a} + \vec{b}_a + \vec{w}_a \quad (1)$$

$$\vec{\omega}_{out} = \bar{M}_g \vec{\omega} + \vec{b}_g + \bar{G}_g \vec{a} + \vec{w}_g \quad (2)$$

Here, $\vec{a}_{out}$ is the 3-axis accelerometer output, $\bar{M}_a$ is the accelerometer scale factor and cross-coupling error matrix, $\vec{a}$ is the 3-axis acceleration input, $\vec{b}_a$ is the accelerometer bias, $\vec{w}_a$ is the accelerometer random noise, $\vec{\omega}_{out}$ is the 3-axis gyroscope output, $\bar{M}_g$ is the gyroscope scale factor and cross-coupling error matrix, $\vec{\omega}$ is the 3-axis rotation input, $\vec{b}_g$ is the gyroscope bias, $\bar{G}_g$ is the gyroscope vibration induced error, $\vec{w}_g$ is the gyroscope random noise [2]. Knowing the cross coupling and bias terms allows one to make the following corrections:

$$\begin{aligned} \vec{a}_{corrected} &= \bar{M}_a^{-1}(\vec{a}_{out} - \vec{b}_a) \\ &\approx \bar{M}_a^{-1}\vec{a}_{out} - \vec{b}_a \end{aligned} \quad (3)$$

$$\begin{aligned} \vec{\omega}_{corrected} &= \bar{M}_g^{-1}(\vec{\omega}_{out} - \vec{b}_g - \bar{G}_g\vec{a}) \\ &\approx \bar{M}_a^{-1}\vec{\omega}_{out} - \vec{b}_g - \bar{G}_g\vec{a} \end{aligned}, \quad (4)$$

with accuracies limited by the random noise $\vec{w}_a$ and $\vec{w}_g$.

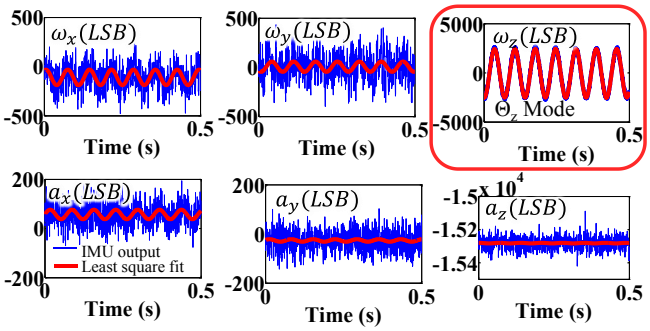

Figure 5: An example of time domain output of 6-axis IMU in Ω_z mode at 15 Hz

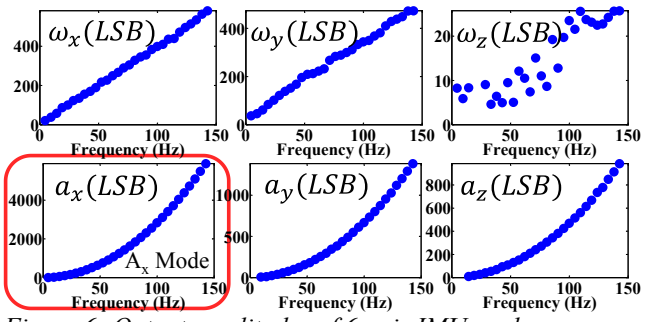

Figure 6: Output amplitudes of 6-axis IMU mode versus input sine frequency in A_x mode

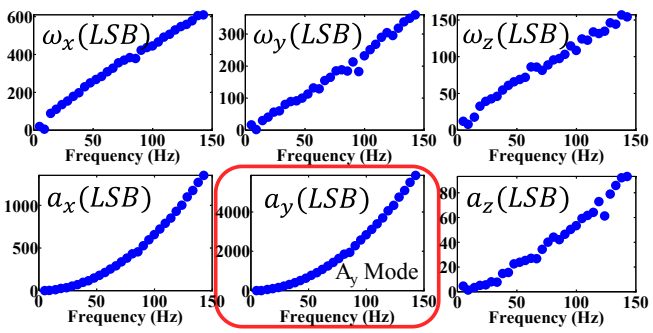

Figure 7: Output amplitudes of 6-axis IMU mode versus input sine frequency in A_y mode

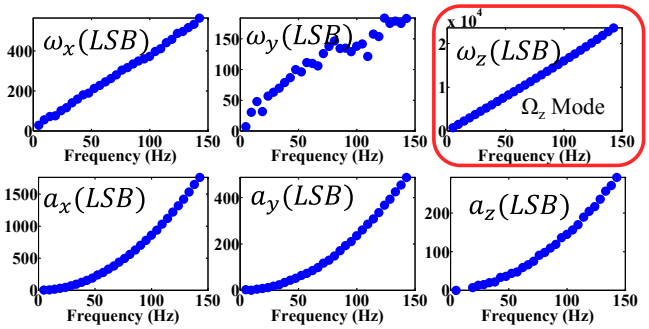

Figure 8: Output amplitudes of 6-axis IMU mode versus input sine frequency in Ω_z mode

In order to extract scale factors, output data rate of the IMU is set at 2 kHz, and 6 axis data are acquired. During this calibration process, the dithering frequency is swept, at constant amplitude, from 5 to 150 Hz in steps of 5 Hz. The IMU output full scale is set to ±125 °/s for gyroscope and ±2g for accelerometer. For each dither frequency, the raw data is recorded in MBED for 0.5 seconds, and sent to MATLAB. For each axis of actuation, all of the 6 axis signals are measured. The time domain output is least square fitted to extract amplitude. An example for the IMU output from Ω_z mode dither at 15 Hz is shown Figure 5. The extracted amplitude of the 6 axis output as a function of sweep frequency for A_x, A_y, and Ω_z modes are shown in Figure 6-8, respectively. In order to extract scale factor, the amplitude in Figure 6-8 is least square fitted by a linear and a quadratic model for gyroscope and accelerometer, respectively, as shown in Table 3-4.

Table 3. Extracted linear coefficient from IMU output for gyroscope.

Dither Mode	Gyroscope coefficient (LSB/Hz)		
	X-axis	Y-axis	Z-axis
A_x	3.97±0.05	3.18±0.07	0.18±0.03
A_y	4.2±0.2	2.5±0.1	1.03±0.05
Ω_z	3.76±0.06	1.1±0.1	164±2

Table 4. Extracted quadratic coefficient from IMU output for accelerometer.

Dither Mode	Accelerometer coefficient (LSB/Hz²)		
	X-axis	Y-axis	Z-axis
A_x	0.288± 0.001	0.0677± 0.0002	0.0478± 0.0003
A_y	0.0663± 0.0004	0.287± 0.002	0.0044± 0.0003
Ω_z	0.0864± 0.0004	0.0240± 0.0002	0.0142± 0.0002

From the calibrated stage scale factor in Table 2, and IMU output coefficient in Table 3-4, the scale factor can be extracted. For example, the calibrated ω_z gyroscope scale factor from PZT dither stage is 0.662/164 (°/s)/LSB. The accelerometer output from the IMU is measured and compared between excitation from PZT dither stage and Vibration Research VR2500 vibration controller and shaker as shown in Figure 9a. The gyroscope output is also measured and compared between excitation from PZT

dither stage and Ideal Aerosmith 12700VS rate table as shown in Figure 9b. The calibrated IMU sensitivities (1/scale factor) from different methods are listed in Table 5 and show gyroscope and accelerometer scale factors that are within 3.3% and 6.7% of their datasheet specifications, respectively. Moreover, from Table 4, gyroscope cross axis sensitivity calibrated by the PZT dither stage is 2.4%, which is within the IMU specification (±5%).

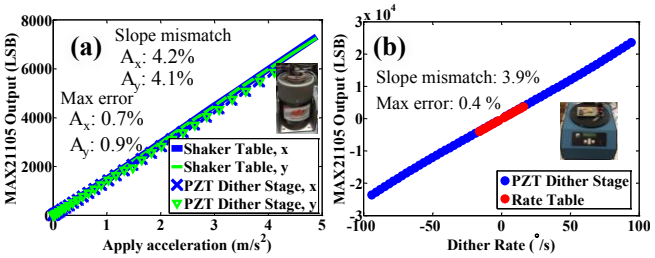

Figure 9: (a) Measured output of a_x and a_y accelerometer in MAX21105 using PZT dither stage and Vibration Research VR2500 vibration controller and shaker. Inset shows photo of the experimental setup. (b) Measured scale factor of ω_z gyroscope in MAX21105 using PZT dither stage, and Ideal Aerosmith 12700VS rate table with 1000 ppm rate repeatability. Inset shows photo of the experimental setup.

Table 5. Calibrated IMU sensitivity (1/scale factor)

	Datasheet	Shaker/Rate Table	PZT dither stage	Unit
a_x	15.0 ± 0.4	14.65 ± 0.05	14.03 ± 0.05	LSB/mg
a_y	15.0 ± 0.4	14.6 ± 0.1	14.0 ± 0.1	LSB/mg
ω_z	240 ± 6	238.7 ± 0.7	248 ± 2	LSB /(°/s)

CONCLUSIONS AND FUTURE WORK

We demonstrated the use of a miniature high bandwidth piezoelectric dither stage to calibrate in plane acceleration and angular dither of a commercial IMU, MAX21105. Extracted gyroscope and accelerometer scale factors are within 3.3 % and 6.7% of their specifications, showing the applicability of our multi-axis calibration system. The system is portable, self-contained, and can potentially be used for *in situ* calibration and correction tool for any commercial IMU MEMS die. Further work is needed to decouple the micro stage motion aging and frequency accuracy of the dither stage to improve measurement accuracy and stability. Our future work involves using new algorithms, coupled with Kalman filters, implemented in a microcontroller or an FPGA to compensate for drift in IMU parameters, while showing improvement in long term navigation accuracy.

ACKNOWLEDGEMENTS

We acknowledge Defense Advanced Research Projects Agency (DARPA), PASCAL program, for funding this work. This work was performed in part at the Cornell NanoScale Facility, a member of the National Nanotechnology Coordinated Infrastructure (NNCI), which is supported by the National Science Foundation (Grant ECCS-15420819). We also acknowledge Prof. Sunil Bhave for the rate table access.

REFERENCES

[1] D. Cardarelli, "An integrated MEMS inertial measurement unit", *IEEE Position Location and Navigation Symposium 2003*, pp. 314-319, 2002.

[2] P. D. Groves, *Principles of GNSS, Inertial, and Multisensor Integrated Navigation Systems*, Artech House, 2013.

[3] N. Sheimy, X. Niu, "The Promise of MEMS to the Navigation Community", *Inside GNSS*, 2007.

[4] T. Olbrich, A. Richardson, W. Vermeiren, B. Straube, "Integrating testability into microsystems", *Microsystem Technologies*, vol. 3, pp. 72-79, 1997.

[5] T. Dong-Si, A.I. Mourikis, "Estimator initialization in vision-aided inertial navigation with unknown camera-IMU calibration," *Intelligent Robots and Systems (IROS)*, pp.1064-1071, 2012.

[6] S. Sukkarieh, E.M. Nebot, H.F. Durrant-Whyte, "A high integrity IMU/GPS navigation loop for autonomous land vehicle applications", *Robotics and Automation, IEEE Transactions*, vol.15, no.3, pp.572-578, 1999.

[7] M. Tanigawa, H. Luinge, L. Schipper, P. Slycke, "Drift-free dynamic height sensor using MEMS IMU aided by MEMS pressure sensor", *Positioning, Navigation and Communication*, pp.191-196, 2008.

[8] W. T. Fong, S. K. Ong, A. Y. C. Nee "Methods for in-field user calibration of an inertial measurement unit without external equipment", *Meas. Sci. Technol.* vol. 19 pp. 85202-85213, 2008.

[9] R. Puers, S. Reyntjens, "RASTA—real-acceleration-for-self-test accelerometer: a new concept for self-testing accelerometers", *Sensors and Actuators A: Physical*, vol. 97–98, pp. 359–368, 2002.

[10] S. Nadig, V. Pinrod, S. Ardanuç, A. Lal, "Multi-modal mechanical stimuli stage for in-situ calibration of MEMS gyroscopes", *2015 IEEE International Symposium on Inertial Sensors and Systems (ISISS)*, 23-26 March 2015, pp. 1-2.

[11] E.E. Aktakka, Jong-Kwan Woo, D. Egert, R.J.M. Gordenker, K. Najafi, "A Microactuation and Sensing Platform With Active Lockdown for In Situ Calibration of Scale Factor Drifts in Dual-Axis Gyroscopes", *IEEE/ASME Transactions on Mechatronics*, vol. 20, no. 2, pp. 934-943, 2015.

[12] S. Nadig, S. Ardanuc, A. Lal, "Monolithic piezoelectric in-plane motion stage with low cross-axis-coupling", *IEEE Micro Electro Mechanical Systems (MEMS)*, 26-30 Jan. 2014, pp. 524-527.

[13] S. Nadig, S. Ardanuc, B. Clark, A. Lal, "DOME-DISC: Diffractive optics metrology enabled dithering inertial sensor calibration," *IEEE Micro Electro Mechanical Systems (MEMS)*, 26-30 Jan. 2014, pp.608-611.

[14] S. Nadig, S. Ardanuc, A. Lal, "Planar Laser-Micro Machined Bulk PZT Bimorph for In-Plane Actuation," *IEEE Transactions on Joint Ultrasonics, Ferroelectrics and Frequency Control (UFFC), EFTF and PFM symposium*, 2013.

CONTACT

V. Pinrod, tel: +1-401-5274425; vp239@cornell.edu